

AD-A115 986

MISSION RESEARCH CORP ALBUQUERQUE NM

F/S 20/14

STANDING WAVES AND NOTCHES IN A PARALLEL-PLATE TYPE OF EMP SIMU--ETC(U)

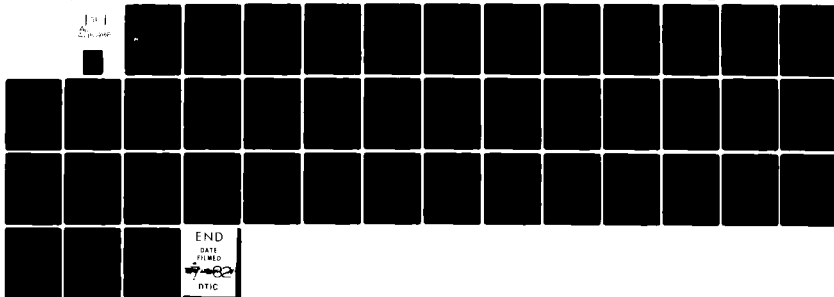
MAR 81 T T WU, R W KING, D J BLEJER, M OWENS F29601-78-C-0082

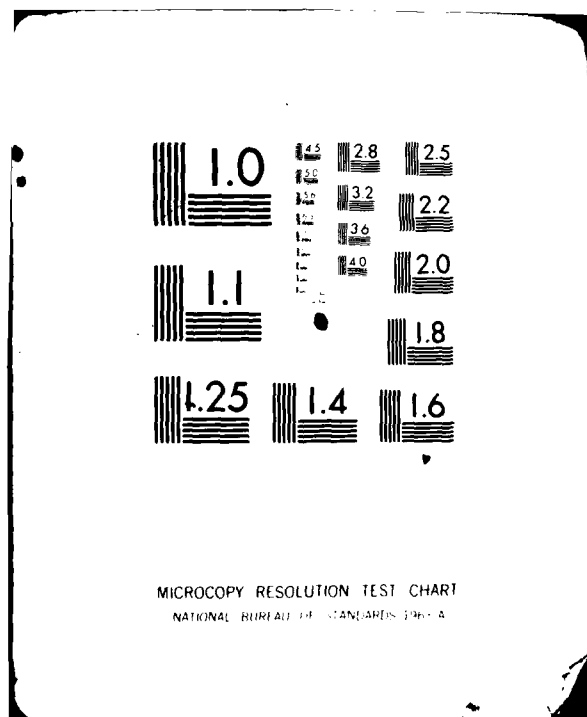
UNCLASSIFIED

AFWL-TR-80-162

NL

101  
S. 101





AFWL-TR-80-162

AFWL-TR-  
80-162

**STANDING WAVES AND NOTCHES  
IN A PARALLEL-PLATE TYPE OF EMP SIMULATOR  
AND THEIR REDUCTION**

T. T. Wu, et al

Mission Research Corporation  
1400 San Mateo Blvd, NE  
Albuquerque, New Mexico 87108

March 1981

Final Report

Approved for public release; distribution unlimited.

**AIR FORCE WEAPONS LABORATORY**  
Air Force Systems Command  
Kirtland Air Force Base, NM 87117

DTIC FILE COPY AD A115986



This final report was prepared by Mission Research Corporation, Albuquerque, New Mexico, under Contract F29601-78-C-0082, Job Order 37630132 with the Air Force Weapons Laboratory, Kirtland Air Force Base, New Mexico. Dr Michael G. Harrison (NTYEI) was the Laboratory Project Officer-in-Charge.

When US Government drawings, specifications, or other data are used for any purpose other than a definitely related Government procurement operation, the Government thereby incurs no responsibility nor any obligation whatsoever, and the fact that the Government may have formulated, furnished, or in any way supplied the said drawings, specifications, or other data, is not to be regarded by implication or otherwise, as in any manner licensing the holder or any other person or corporation, or conveying any rights or permission to manufacture, use, or sell any patented invention that may in any way be related thereto.

This report has been authored by a contractor of the United States Government. Accordingly, the United States Government retains a nonexclusive, royalty-free license to publish or reproduce the material contained herein, or allow others to do so, for the United States Government purposes.

This report has been reviewed by the Public Affairs Office and is releasable to the National Technical Information Service (NTIS). At NTIS, it will be available to the general public, including foreign nations.

This technical report has been reviewed and is approved for publication.

*Michael G. Harrison*

MICHAEL G. HARRISON, PhD  
Project Officer

FOR THE COMMANDER

*J. Philip Castillo*  
J. PHILIP CASTILLO, PhD  
Chief, Electromagnetics Branch

*Norman K. Blocker*  
NORMAN K. BLOCKER  
Colonel, USAF  
Chief, Applied Physics Division

DO NOT RETURN THIS COPY. RETAIN OR DESTROY.

UNCLASSIFIED

SECURITY CLASSIFICATION OF THIS PAGE (When Data Entered)

REPORT DOCUMENTATION PAGE		READ INSTRUCTIONS BEFORE COMPLETING FORM
1. REPORT NUMBER AFWL-TR-80-162	2. GOVT ACCESSION NO. <b>AD-A115 986</b>	3. RECIPIENT'S CATALOG NUMBER
4. TITLE (and Subtitle) STANDING WAVES AND NOTCHES IN A PARALLEL-PLATE TYPE OF EMP SIMULATOR AND THEIR REDUCTION		5. TYPE OF REPORT & PERIOD COVERED Final Report
7. AUTHOR(s) T. T. Wu R. W. P. King		8. CONTRACT OR GRANT NUMBER(s) F29601-78-C-0082
9. PERFORMING ORGANIZATION NAME AND ADDRESS Mission Research Corporation 1400 San Mateo Blvd, SE Albuquerque, New Mexico 87108		10. PROGRAM ELEMENT, PROJECT, TASK AREA & WORK UNIT NUMBERS 64711F/37630132
11. CONTROLLING OFFICE NAME AND ADDRESS Air Force Weapons Laboratory (NTYEI) Kirtland Air Force Base, New Mexico 87117		12. REPORT DATE March 1981
14. MONITORING AGENCY NAME & ADDRESS (if different from Controlling Office)		13. NUMBER OF PAGES 40
		15. SECURITY CLASS. (of this report) UNCLASSIFIED
		15a. DECLASSIFICATION/DOWNGRADING SCHEDULE
16. DISTRIBUTION STATEMENT (of this Report) Approved for public release; distribution unlimited.		
17. DISTRIBUTION STATEMENT (of the abstract entered in Block 20, if different from Report)		
18. SUPPLEMENTARY NOTES		
19. KEY WORDS (Continue on reverse side if necessary and identify by block number) EMP Model Simulator Mid-frequency Range Electric Field in Parallel-Plate Region Standing-Wave Ratio (SWR) Deep Minimum or Notch Effect of Terminating Resistance Bifurcating Metal or Resistive Sheet Resistive Modal Filter Series Apron or Folded Section		
20. ABSTRACT (Continue on reverse side if necessary and identify by block number) The high standing-wave ratio (SWR) in a model simulator in the mid-frequency range defined by $kh = 2\pi h/\lambda \sim 2\pi$ (where $h$ is the height of the parallel-plate region) is investigated experimentally. It is shown that the isolated deep minimum or notch is due to the mutual cancellation of the imaginary parts of the $TM_{01}$ and TEM modes. The effects on the SWR and the deep minimum of changes in the magnitude and location of the terminating resistance are investigated. Also studied are the introduction of a bifurcating plate, resistive modal filters, (Continued)		

DD FORM 1 JAN 73 1473

UNCLASSIFIED

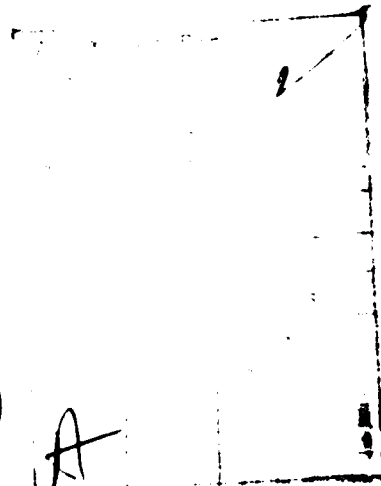
SECURITY CLASSIFICATION OF THIS PAGE (When Data Entered)

UNCLASSIFIED

SECURITY CLASSIFICATION OF THIS PAGE(When Data Entered)

Block No. 20 (Continued)

and series aprons. It is shown that with the proper adjustment of the last named, the *notch* can be eliminated and the SWR reduced to near two at discrete frequencies that span the entire mid-frequency range. Since the low-frequency ranges already have low SWRs, the simulator has been made effective over the entire frequency band in the sense that the SWR is low.



UNCLASSIFIED

SECURITY CLASSIFICATION OF THIS PAGE(When Data Entered)

## SUMMARY

EMP simulators consisting of a central parallel-plate region and tapered input and load sections are well known to provide a high quality of simulation of an incident plane wave at all frequencies for which the spacing of the parallel plates is a small fraction of the wavelength. In this range, the electromagnetic properties of the simulator are those of the well understood two-conductor transmission line in which TEM waves propagate from the generator to the terminating impedance, radiation from the structure is negligible, and reflections at the junctions of the tapered and parallel-plate sections are insignificant. When the terminating impedance is equal to the characteristic impedance of the structure, the standing-wave ratio (SWR) is small, and most of the power supplied by the generator is dissipated in the termination.

At higher frequencies for which the wavelengths of interest are comparable with the parallel-plate spacing, radiation becomes a dominant instead of negligible property of the structure which now behaves more like an antenna than a transmission line. Significant reflections occur at the junctions of the parallel-plate and tapered sections and at their edges so that only a small fraction of the input power actually reaches the terminating load. Most of it is radiated since the electromagnetic field, instead of being bound quite close to the conductors, now extends far out in space. The representation of the field between the parallel plates by a TEM mode becomes inadequate, and higher modes are required. An earlier experimental study of the field in the Harvard model simulator at the high frequency  $f = 625$  MHz showed that, due to strong radiation loading when the plate spacing ( $h$ ) is greater than a wavelength, the SWR in the parallel-plate region was quite low (less than 2.0).

In an intermediate frequency range when  $h \lesssim \lambda$ , neither the transmission-line termination nor the radiation loading is effective in maintaining a low SWR in the parallel-plate region. In particular, when  $f = 271$  MHz and  $h = 75$  cm  $= 0.67\lambda$ , the SWR is generally of the order of 5 to 6 and, in addition, a very deep minimum (notch) is observed with an associated SWR as high as 25. An experimental investigation has been conducted to study the electric field throughout the parallel-plate region of the

Harvard model simulator at  $f = 271$  MHz. Attention was directed to determining the origin of the deep minimum and to devising means for eliminating it and reducing the otherwise quite high SWR.

The study shows that the isolated deep minimum or "notch" is due to the mutual cancellation of the imaginary parts of the  $TM_{01}$  and TEM modes. The effects on the SWR and the deep minimum of changes in the magnitude and location of the terminating resistance are investigated. Also studied are the introduction of a bifurcating plate, resistive modal filters, and series aprons. With the proper adjustment of the last named, the "notch" can be eliminated and the SWR reduced to near two over the entire mid-frequency range. Since the low-frequency and high-frequency ranges already have low SWR's, the simulator has been made effective over the entire frequency band in the sense that the SWR is low.



## CONTENTS

<u>Section</u>		<u>Page</u>
I	INTRODUCTION	7
II	STANDING WAVES AND THE DEEP MINIMUM; EFFECT OF MAGNITUDE AND LOCATION OF TERMINATING RESISTANCE	12
III	SELECTIVE REFLECTION AND ABSORPTION OF THE TM MODE	26
IV	REDUCTION OF THE SWR OF THE TEM MODE	32
V	CONCLUSION	37
	LIST OF PUBLICATIONS	39

# ILLUSTRATIONS

Figure		Page
1	The Harvard model simulator adjusted for intermediate frequencies ( $f \sim 271$ MHz).	8
2	Measured magnitude of the transverse magnetic field at a fixed position in the working volume as a function of frequency; width $2a = 175$ cm, length $b = 114.8$ cm, height $h = 75$ cm, forward power $p_f = 40$ W.	10
3	Measured magnitude and phase of the transverse component of the magnetic field on the ground plane in the working volume; width $2a = 175$ cm, length $b = 114.8$ cm, height $h = 75$ cm.	11
4	Measured electric field $E_z =  E_z  \exp(i\theta_z) = E_{zR} + iE_{zI}$ ; $\theta_z = 0$ at $x = z = 0$ , $y = -3$ cm on ground plane at center of parallel-plate region.	14
5	Measured electric field $E_z =  E_z  \exp(i\theta_z) = E_{zR} + iE_{zI}$ ; $\theta_z = 0$ at $x = y = z = 0$ on ground plane at center of parallel-plate region.	15
6	Measured electric field $E_z =  E_z  \exp(i\theta_z) = E_{zR} + iE_{zI}$ ; $\theta_z = 0$ at $x = z = 0$ , $y = 2$ cm on ground plane at center of parallel-plate region.	16
7	Measured electric field $E_z =  E_z  \exp(i\theta_z) = E_{zR} + iE_{zI}$ ; $\theta_z = 0$ at $x = z = 0$ , $y = 1$ cm on ground plane at center of parallel-plate region.	17
8	TEM and TM components of the electric field in the parallel-plate region. $(E_z)_{\text{TEM}} = E_z(z/h=0.5)$ ; $(E_z)_{\text{TM}} = E_z(z/h=0) - E_z(z/h=0.5) = E_z(z/h=0.5) - E_z(z/h=1)$ [denoted respectively by $\circ$ and $\times$ in graph for $(E_z)_{\text{TM}}$ ]. $E_z =  E_z  \exp(i\theta_z) = E_{zR} + iE_{zI}$ ; $\theta_z = 0$ at $x = y = z = 0$ .	20
9	TEM and TM components of the electric field in the parallel-plate region. $(E_z)_{\text{TEM}} = E_z(z/h=0.5)$ ; $(E_z)_{\text{TM}} = E_z(z/h=0) - E_z(z/h=0.5)$ ; $E_z =  E_z  \exp(i\theta_z) = E_{zR} + iE_{zI}$ ; $\theta_z = 0$ at $x = y = z = 0$ .	21
10	TEM and TM components of the electric field in the parallel-plate region. $(E_z)_{\text{TEM}} = E_z(z/h=0.5)$ ; $(E_z)_{\text{TM}} = E_z(z/h=0) - E_z(z/h=0.5)$ ; $E_z =  E_z  \exp(i\theta_z) = E_{zR} + iE_{zI}$ ; $\theta_z = 0$ at $x = z = 0$ , $y = 2$ cm.	22
11	TEM and TM components of the electric field in the parallel-plate region. $(E_z)_{\text{TEM}} = E_z(z/h=0.5)$ ; $(E_z)_{\text{TM}} = E_z(z/h=0) - E_z(z/h=0.5)$ ; $E_z =  E_z  \exp(i\theta_z) = E_{zR} + iE_{zI}$ ; $\theta_z = 0$ at $x = z = 0$ , $y = 1$ cm.	23

<u>Figure</u>		<u>Page</u>
12	Measured electric field $E_z =  E_z  \exp(i\theta_z) = E_{zR} + iE_{zI}$ , $\theta_z = 0$ at $x = z = 0$ , $y = 1$ cm on the ground plane. Bifurcating metal plate extending from $y = 57.5$ to $y = 89.5$ cm, 175 cm wide.	27
13	TEM and TM components of the electric field in the parallel-plate region. $(E_z)_{\text{TEM}} = E_z(z/h = 0.5)$ ; $(E_z)_{\text{TM}} = E_z(z/h = 0) - E_z(z/h = 0.5)$ ; $E_z =  E_z  \exp(i\theta_z) = E_{zR} + iE_{zI}$ ; $\theta_z = 0$ at $x = z = 0$ , $y = 1$ cm. Bifurcated at $z = h/2$ , $y = 57.5$ cm by metal plate (32 cm $\times$ 175 cm).	28
14	Measured magnitude $ E_z(0,y,0) $ of the electric field in the parallel-plate region; $f = 271$ MHz, $b = 114.8$ cm, $h = 75$ cm, $R = 86 \Omega$ , $y_R = 376$ cm.	30
15	Cross section of Harvard simulator with sleeve or apron sections.	34
16	Measured field in parallel-plate region with and without folded section.	35

# TABLE

<u>Table</u>		<u>Page</u>
1	Maximum SWR for $B_x$ in parallel-plate region; $250 \text{ MHz} \leq f \leq 275 \text{ MHz}$ , $-0.2b \leq y \leq 0.2b$ .	19

## I. INTRODUCTION

In order to approximate an electromagnetic pulse propagating outward in the atmosphere at a sufficient distance from a nuclear explosion, the electromagnetic field in a simulator of the guided-wave type (ref. 1) shown in Figure 1 must have the properties of a simple TEM wave at each frequency in the entire range involved in the pulse. In particular, the standing-wave ratio (SWR) must be close to unity throughout the volume bounded by the parallel-plate part of the simulator. It is well known and readily verified that in the low-frequency part of the spectrum defined by  $kh = 2\pi h/\lambda \ll 1$ , where  $h$  is the height of the parallel-plate section above the ground plane, the SWR is very small when the terminating resistance  $R$  at the load end of the simulator is made equal to the characteristic resistance  $R_c$  of the simulator. In this range, radiation from the structure is negligible so that conventional transmission-line theory applies. Virtually all of the power supplied at the input terminals is dissipated in the terminating resistance.

It was shown in a recent paper (ref. 2) that the SWR is also quite low in the high-frequency range defined by  $kh = 2\pi h/\lambda > 2\pi$ . The relevant measurements were made in the Harvard model simulator specifically at  $f = 625$  MHz with  $h = 108$  cm  $= 2.25\lambda$  or  $kh = 4.5\pi = 14.1$ . In this range, dissipation in the terminating resistance is very small and most of the power supplied at the input terminals is radiated, as from an electromagnetic horn that is well-matched to space. When  $kh > 1$ , conventional transmission-line theory - which assumes radiation to be negligible - is inadequate.

At intermediate frequencies when  $kh \sim 2\pi$ , the power radiated and the power dissipated in the terminating resistance are of comparable magnitude. Also the effective condition of match deteriorates so that a large SWR is observed. Under special circumstances at certain critical frequencies and

1. Baum, C. E., "EMP Simulators for Various Types of Nuclear EMP Environments: An Interim Categorization," IEEE Trans. Antennas Propagat., AP-26, pp. 35-53, 1978.
2. King, R. W. P., and Blejer, D. J., "The Electromagnetic Field in an EMP Simulator at a High Frequency," IEEE Trans. Electromagn. Compatib., EMC-21, pp. 263-269, 1979.

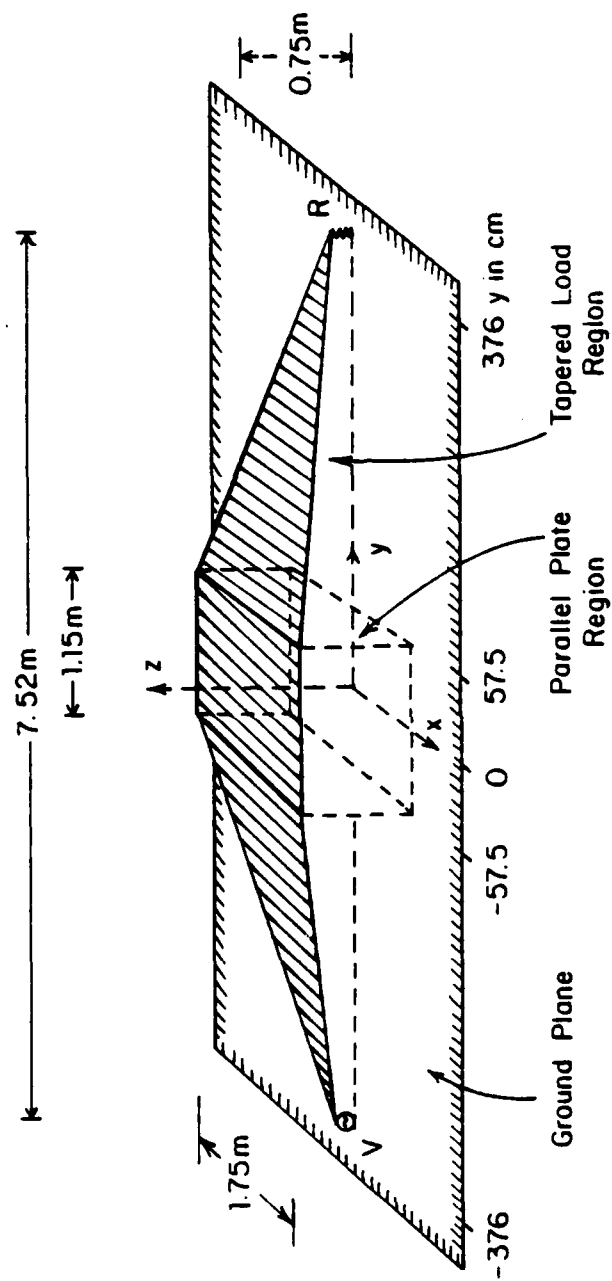


Figure 1. The Harvard model simulator adjusted for intermediate frequencies  
( $f \sim 271 \text{ MHz.}$ )

locations, unusually deep minima occur in the standing-wave pattern. The ratio of an adjacent maximum to such a deep minimum may be as large as 25. An example of such a deep minimum or "notch" is shown in Figure 2 in terms of the measured magnitude of the transverse magnetic field  $H_x(x,y,z)$  in the parallel-plate region at the point  $x = -10.5$ ,  $y = 8.5$ ,  $z = 0$  cm as a function of frequency. It is seen that there is a succession of minima and maxima but only one very deep minimum at  $f = 264$  MHz. This has been called the "notch." At another location in the simulator, the frequency for and the depth of the deepest minimum are different. This is illustrated in Figure 3 which shows the standing-wave pattern of  $H_x(x,y,z)$  at several frequencies. It may be added that the associated deep minima for  $E_z(x,y,z)$  occur at locations that are displaced by axial distances near  $\lambda/4$  from the minima for  $H_x(x,y,z)$ . The deepest minimum for  $E_z(x,y,z)$  occurs at  $f = 271$  MHz.

It is the purpose of this investigation to study the electric field throughout the parallel-plate region of the model simulator at  $f = 271$  MHz in order to discover the origin of the generally high SWR and of the deep minimum. A further purpose is the elimination of the deep minimum and the reduction of the SWR to acceptable levels. If this is accomplished, the simulator can better serve its intended purpose.

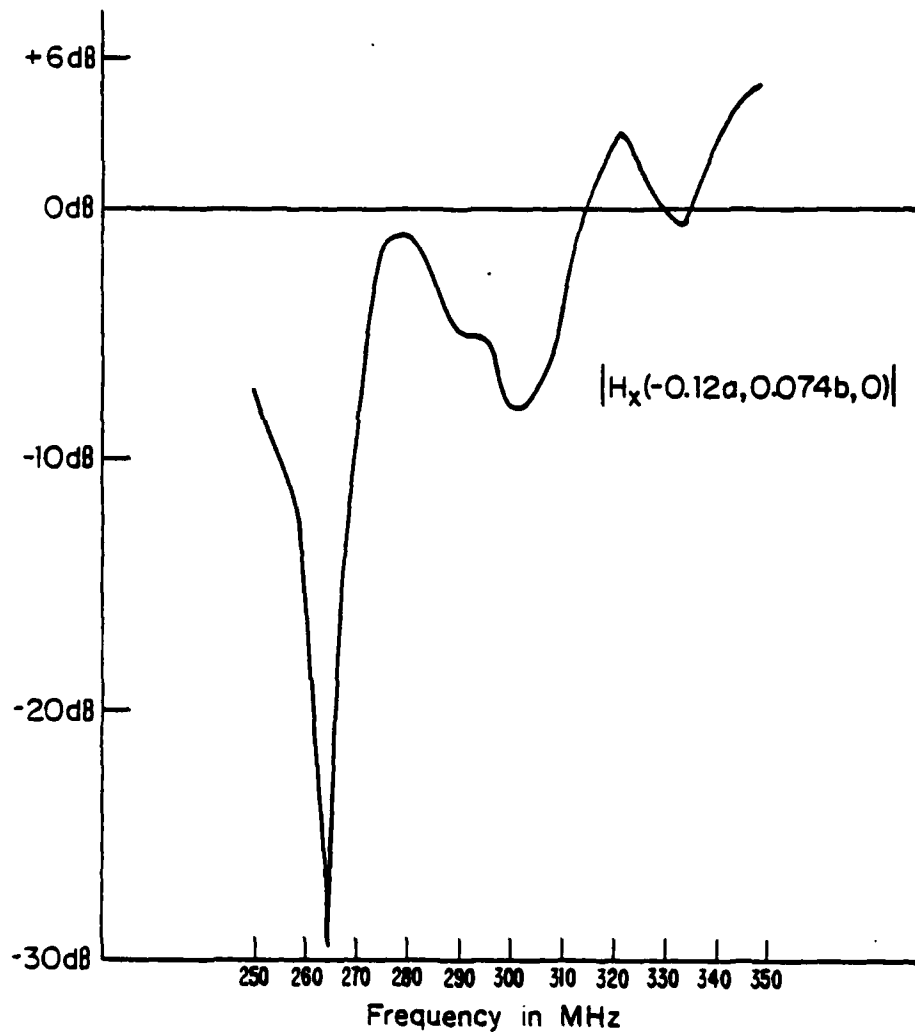


Figure 2. Measured magnitude of the transverse magnetic field at a fixed position in the working volume as a function of frequency; width  $2a = 175$  cm, length  $b = 114.8$  cm, height  $h = 75$  cm, forward power  $p_f = 40$  W.



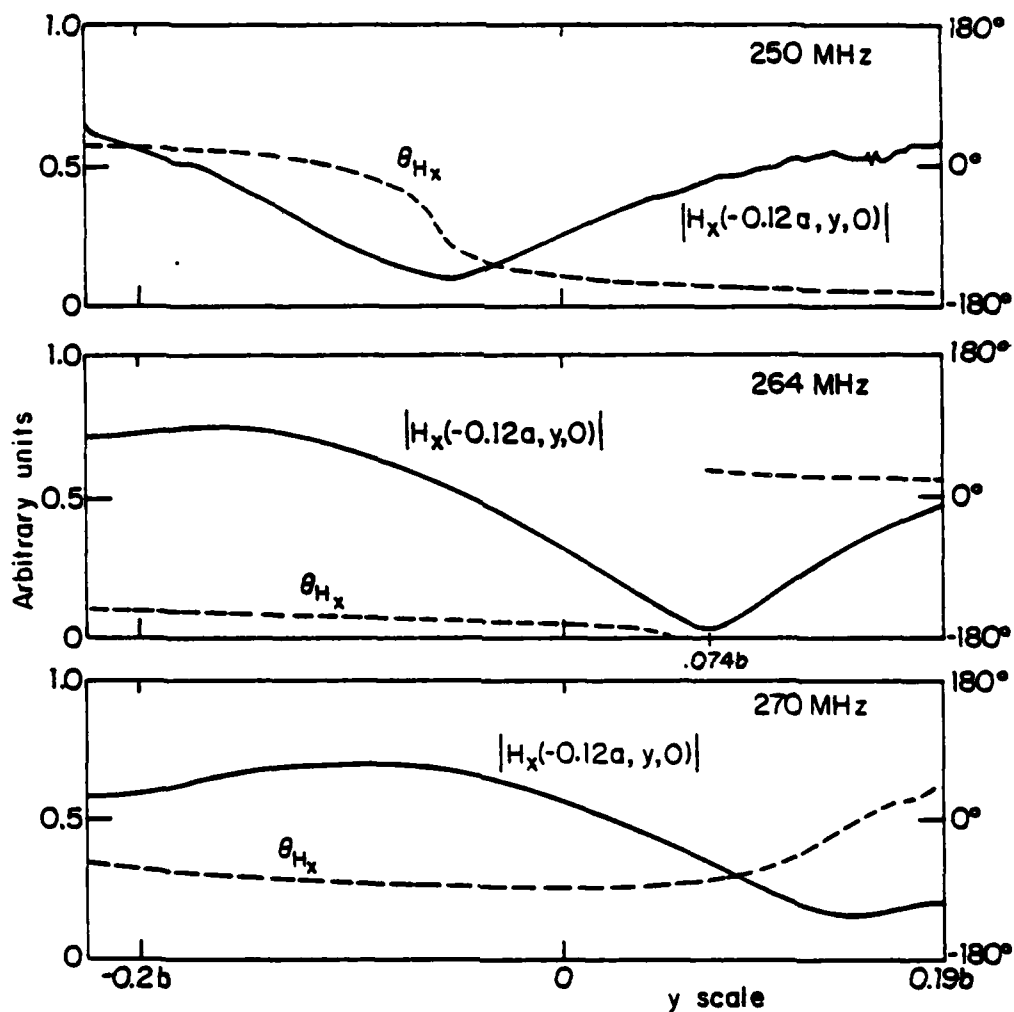


Figure 3. Measured magnitude and phase of the transverse component of the magnetic field on the ground plane in the working volume; width  $2a = 175$  cm, length  $b = 114.8$  cm, height  $h = 75$  cm.

## II. STANDING WAVES AND THE DEEP MINIMUM; EFFECT OF MAGNITUDE AND LOCATION OF TERMINATING RESISTANCE

An analysis of the standing-wave patterns of the electromagnetic field in the critical intermediate range of frequencies has been carried out in the Harvard model simulator described in detail in reference 2 (Figures 1 and 2). For the present study the frequency has been lowered from 625 MHz to 271 MHz and the height  $h$  of the central parallel-plate section (length  $b = 114.8$  cm, width  $2a = 175$  cm) has been decreased from  $h = 108$  cm to  $h = 75$  cm. With this height, only the TEM and  $TM_{01}$  modes can propagate and these two components are readily separated experimentally. These modes are defined and analytically represented in reference 2. Attention is directed only to the field in a range near the central plane  $x = 0$  in which contributions by TE modes are negligible.

In order to investigate the SWR and the deep minimum, measurements were made of  $E_z = |E_z| \exp(i\theta_z) = E_{zR} + iE_{zI}$  and of  $E_y = |E_y| \exp(i\theta_y) = E_{yR} + iE_{yI}$  in the central plane  $x = 0$  throughout the parallel-plate region which extends from  $y = -57.5$  cm to  $y = 57.5$  cm and from  $z = 0$  to  $z = h = 75$  cm. Of particular interest are: the field at  $z = 0$  on the ground plane where  $E_z(0, y, 0) = [E_z(0, y, 0)]_{TEM} + [E_z(0, y, 0)]_{TM}$  and  $E_y(0, y, 0) = [E_y(0, y, 0)]_{TM} = 0$ ; the field at  $z = h/2$  where  $E_z(0, y, h/2) = [E_z(0, y, h/2)]_{TEM}$  with  $[E_z(0, y, h/2)]_{TM} = 0$  and  $E_y(0, y, h/2) = [E_y(0, y, h/2)]_{TM}$ ; and the field at  $z = h$  where  $E_z(0, y, h) = [E_z(0, y, h)]_{TEM} - [E_z(0, y, h)]_{TM}$  and  $E_y(0, y, h) = [E_y(0, y, h)]_{TM} = 0$ . It follows that the amplitudes of the TEM and TM components are:  $(E_z)_{TEM} = E_z(0, y, h/2)$ ;  $(E_z)_{TM} = E_z(0, y, 0) - E_z(0, y, h/2) = E_z(0, y, h/2) - E_z(0, y, h)$ ; and  $(E_y)_{TM} = E_y(0, y, h/2)$ . Thus, it is sufficient to measure  $E_z(0, y, 0)$ ,  $E_z(0, y, h/2)$ , and  $E_y(0, y, h/2)$  as functions of  $y$  in order to be able to represent graphically  $(E_z)_{TEM}$ ,  $(E_z)_{TM}$ , and  $(E_y)_{TM}$  as functions of  $y$ . In carrying out the measurements with the probe systems described in reference 2, the phase of the field is referred to a point as close to  $x = y = z = 0$  as conveniently possible.

A standing wave in the parallel-plate region is necessarily due both to partial reflection of the total current at the junction of the parallel plate and the sloping tapered plate where radiation occurs, and to more or less continuous reflection along the tapered section to the cut-off height

for the current associated with the  $TM_{01}$  mode. Only currents associated with the TEM mode reach the terminating resistance where a negligible reflection takes place when  $R = R_c$ . In order to study the standing waves in the parallel-plate region, it is useful to determine the distribution of  $E_z$  with  $R \sim R_c$  at two locations, viz., at the end  $y_R = 376$  cm of the tapered section and at  $y_R = 376 - \lambda/4 \sim 357$  cm, and with  $R \sim 2R_c$  at the same two locations. With these choices, partial reflections of the TEM currents at the termination can be combined in two phase relations with partial reflections of the TEM and TM currents occurring elsewhere.

The magnitude  $|E_z|$  and angle  $\theta_z$  were measured in the plane  $x = 0$  in the parallel-plate region. The phase reference is the center of the ground plane at  $x = y = z = 0$ . Since the phase at this point had to be interpolated from measurements at adjacent points, the actual phase reference in several sets of measurements departs slightly from  $y = 0$ . Graphs of the measured values of  $|E_z|$  and  $E_{zR} = |E_z| \cos \theta_z$ ,  $E_{zI} = |E_z| \sin \theta_z$  at  $f = 271$  MHz are shown in Figures 4 through 7. In these the terminating resistance  $R$  and its location  $y_R$  are given respectively by:  $R \sim 100 \Omega$ ,  $y_R = 376$  cm;  $R \sim 100 \Omega$ ,  $y_R = 357$  cm;  $R \sim 200 \Omega$ ,  $y_R = 376$  cm; and  $R \sim 200 \Omega$ ,  $y_R = 357$  cm. The four sets of graphs are quite similar. All have one minimum of  $|E_z|$  near  $y = -12$  cm and a second much deeper minimum near  $y = 45$  cm; the associated maxima are near  $y = -43$  cm and  $y = 13$  cm. The apparent SWR of the first maximum to the first minimum is smaller, by approximately a factor of 4, than the SWR of the second maximum to the second minimum. This latter has a value in the 20's in Figures 4 through 6 and is 6.9 in Figure 7. As is to be expected, a change in the location of the termination from  $y_R = 376$  cm to  $y_R = 357$  cm has little effect when  $R \sim 100 \Omega \sim R_c$  (Figures 4 and 5), but has a significant effect when  $R \sim 200 \Omega \sim 2R_c$  (Figures 6 and 7).

A second series of measurements, relating in this case to the standing waves in the magnetic field in the parallel-plate region, was made with two different terminating resistances, viz.,  $R = 100 \Omega \sim R_c$  and  $R = 470 \Omega \sim 6R_c$ . The very high SWR near the "notch" frequency with  $R = 100 \Omega$  was substantially reduced with  $R = 470 \Omega$ . This behavior was not significantly altered over the frequency range from 200 MHz to 900 MHz. At  $f = 50$  MHz, the structure behaved substantially like a transmission line with standing-

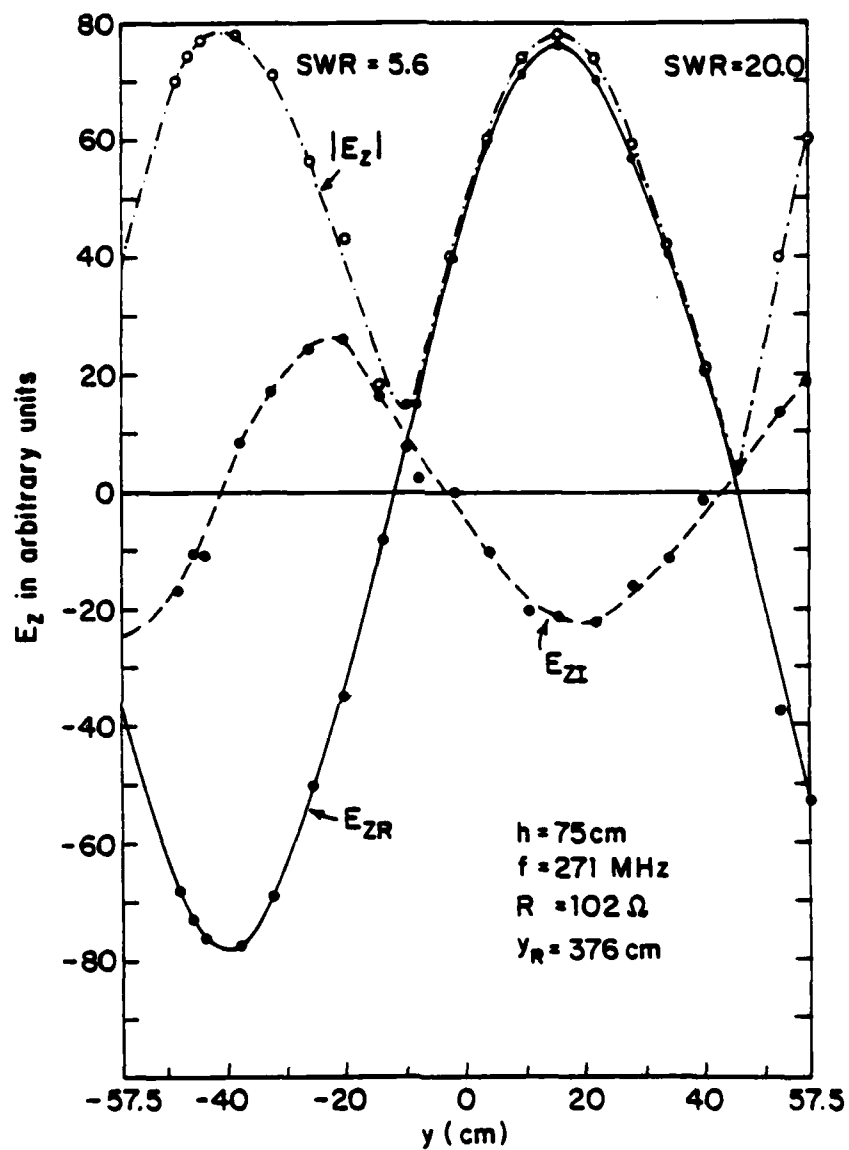


Figure 4. Measured electric field  $E_z = |E_z| \exp(i\theta_z) = E_{zR} + iE_{zI}$ ;  $\theta_z = 0$  at  $x = z = 0$ ,  $y = -3 \text{ cm}$  on ground plane at center of parallel-plate region.

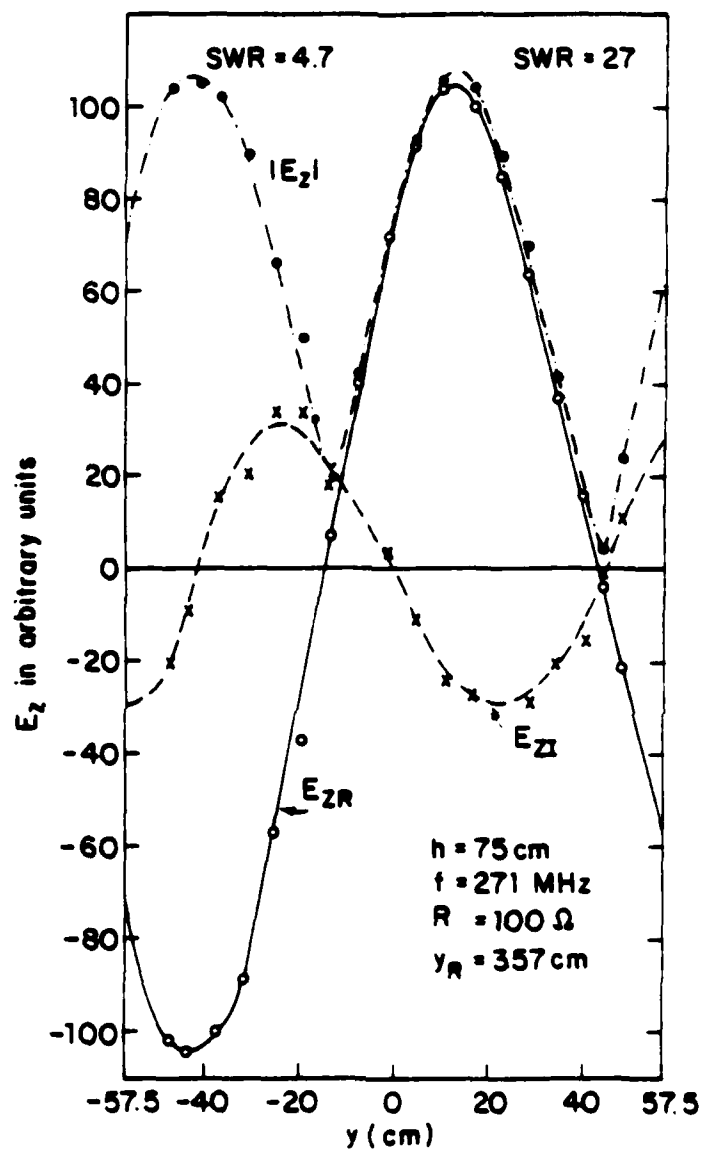


Figure 5. Measured electric field  $E_z = |E_z| \exp(i\theta_z) = E_{zR} + iE_{zI}$ :  
 $\theta_z = 0$  at  $x = y = z = 0$  on ground plane at center of  
parallel-plate region.

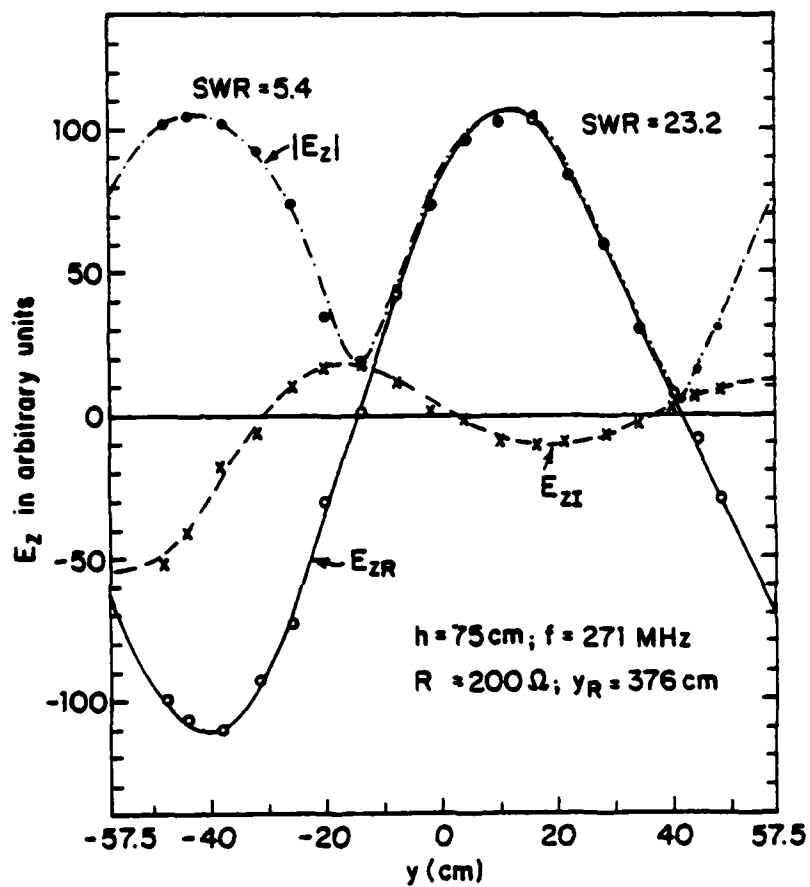


Figure 6. Measured electric field  $E_z = |E_z| \exp(i\theta_z) = E_{zR} + iE_{zI}$ ;  $\theta_z = 0$  at  $x = z = 0$ ,  $y = 2 \text{ cm}$  on ground plane at center of parallel-plate region.

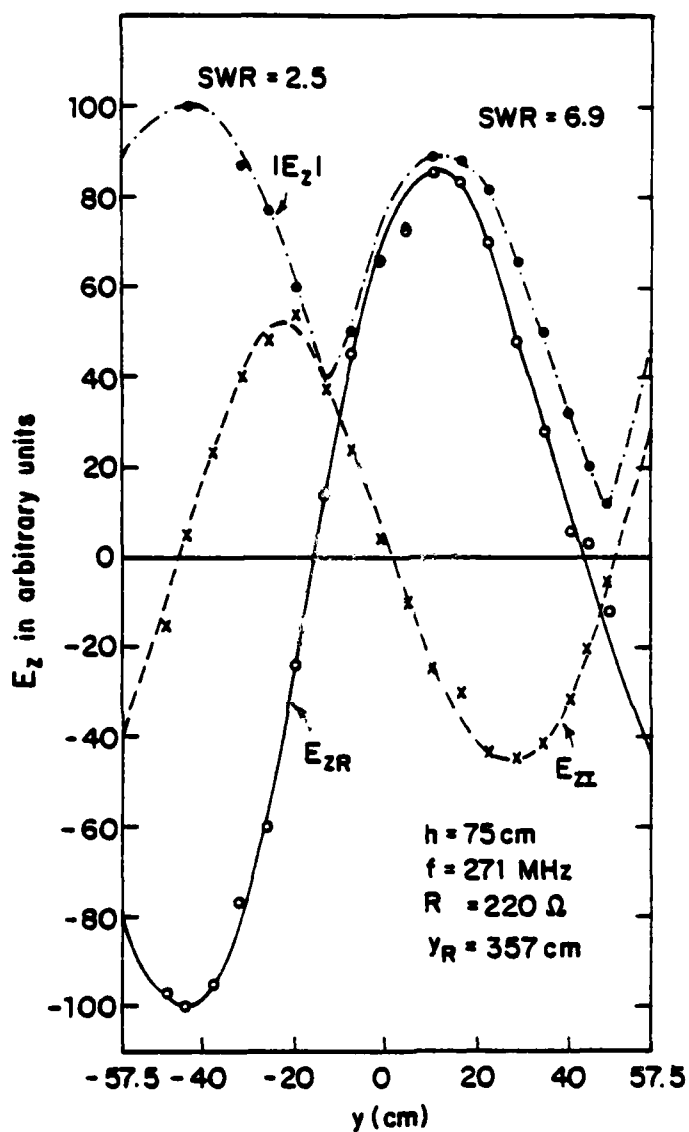


Figure 7. Measured electric field  $E_z = |E_z| \exp(i\theta_z) = E_{zR} + iE_{zI}$ ;  $\theta_z = 0$  at  $x = z = 0$ ,  $y = 1 \text{ cm}$  on ground plane at center of parallel-plate region.

wave distributions correctly given by transmission-line theory. The maximum SWR of the magnetic field  $B_x$  along the axis of the simulator just above the ground plane in the parallel-plate region is shown in Table 1 for three load resistances in the frequency range  $250 \text{ MHz} \leq f \leq 275 \text{ MHz}$ . It is seen that the SWR is consistently high when  $R = 100 \Omega \sim R_c$ ; it is not significantly affected by the location of the terminating resistor since any power that reaches it is dissipated without reflection. When  $R = 220 \Omega$  and  $R = 470 \Omega$ , the SWR is very high when the termination is at  $y_1 = 328 \text{ cm}$  and  $y_3 = 375 \text{ cm} \sim y_1 + \lambda/2$ ; the SWR is quite low when  $y_2 = 357 \text{ cm}$ . Evidently, some of the power that reaches the termination is reflected and combines with other reflections to increase the SWR when  $y = y_1$  and  $y = y_3$  and to decrease it when  $y = y_2$ . This depends on the relative phases and these are determined by the location of the resistor.

In order to investigate the relative importance of the TEM and  $TM_{01}$  modes in maintaining a high SWR, the measured  $E_z$  and  $E_y$  components of the electric field in the parallel-plate region shown graphically in Figures 4 through 7 were resolved into their TEM and  $TM_{01}$  components. At the ground plane,  $E_z(z/h = 0) = (E_z)_{\text{TEM}} + (E_z)_{\text{TM}}$ ; at the top plate,  $E_z(z/h = 1) = (E_z)_{\text{TEM}} - (E_z)_{\text{TM}}$ ; and halfway between the plates,  $E_z(z/h = 0.5) = (E_z)_{\text{TEM}}$ . Also,  $E_y(z/h = 0.5) = (E_y)_{\text{TM}}$  since  $(E_y)_{\text{TEM}} = 0$  everywhere. Since all components are complex, each has a real and an imaginary part referred to the phase at the center of the ground plane. The real and imaginary parts and the magnitude of  $(E_z)_{\text{TEM}}$  are shown at the top in Figures 8 through 11 for the conditions, respectively, of Figures 4 through 7. Both maximum/minimum ratios are quite comparable with each other and with the corresponding first ratio of the total field in Figures 4 through 7. The very large second ratio is due to the very deep second minimum. This is not present with the TEM mode. When  $R \sim R_c \sim 100 \Omega$ , the TEM mode is terminated with no reflection and, hence, with the  $\text{SWR} \sim 1$ . But this is true only when the simulator height  $h$  is a very small fraction of a wavelength and transmission-line theory (which assumes negligible radiation) is a good approximation. When  $h$  is not small compared to the wavelength, the structure is not a simple transmission line but an antenna that radiates like a horn. There are significant reflections at the end of the parallel-plate region and these generate a fairly large SWR. Only a small fraction of the power



TABLE 1. Maximum SWR for  $B_x$  in Parallel-Plate Region;  $250 \text{ MHz} \leq f \leq 275 \text{ MHz}$   
 $-0.2b \leq y \leq 0.2b$

Load Position Resistance	$y_1 = 328 \text{ cm}$	$y_2 = 357 \text{ cm}$	$y_3 = 375 \text{ cm}$
100 $\Omega$	SWR = 14.5 f = 266 MHz	SWR = 12 f = 273 MHz	SWR = 17.5 f = 268 MHz
220 $\Omega$	SWR = 25 f = 270 MHz	SWR = 3.18 f = 270 MHz	(200 $\Omega$ load) SWR = 18.6 f = 268 MHz
470 $\Omega$	SWR = 30 f = 272 MHz	SWR = 3.0 f = 260 MHz	(440 $\Omega$ load) SWR = 24.4 f = 274 MHz

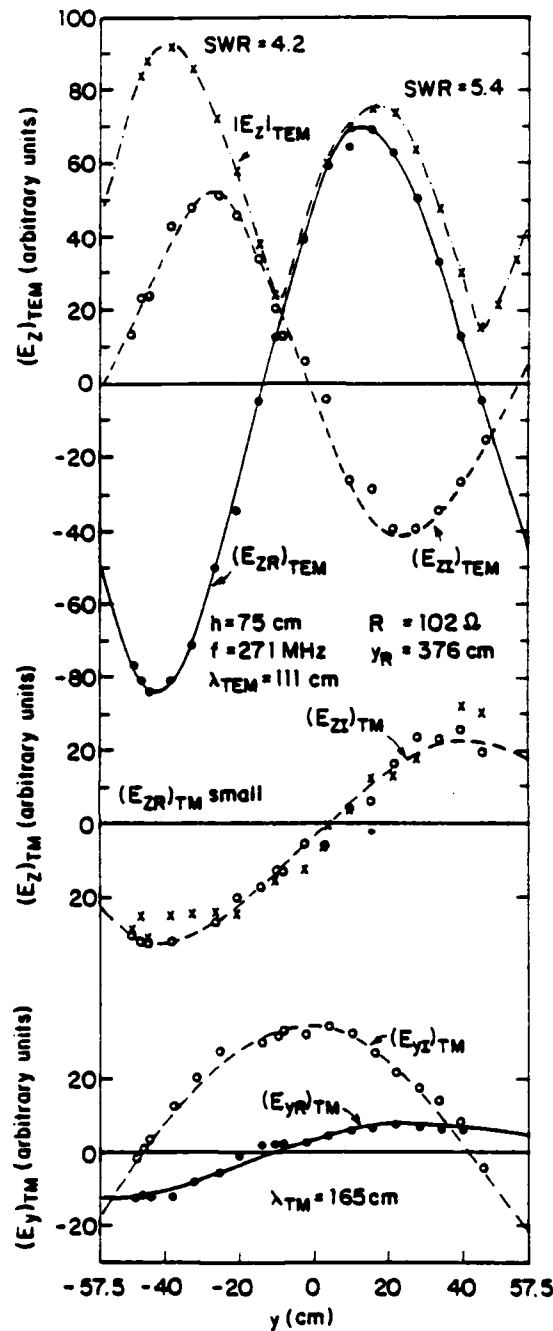


Figure 8. TEM and TM components of the electric field in the parallel-plate region.  $(E_z)_{\text{TEM}} = E_z(z/h=0.5)$   $(E_z)_{\text{TM}} = E_z(z/h=0) - E_z(z/h=0.5) = E_z(z/h=0.5) - E_z(z/h=1)$  [denoted respectively by o and x in graph for  $(E_z)_{\text{TM}}$ ].  $E_z = |E_z| \exp(i\theta_z) = E_{zR} + iE_{zI}$ ;  $\theta_z = 0$  at  $x = y = z = 0$ .

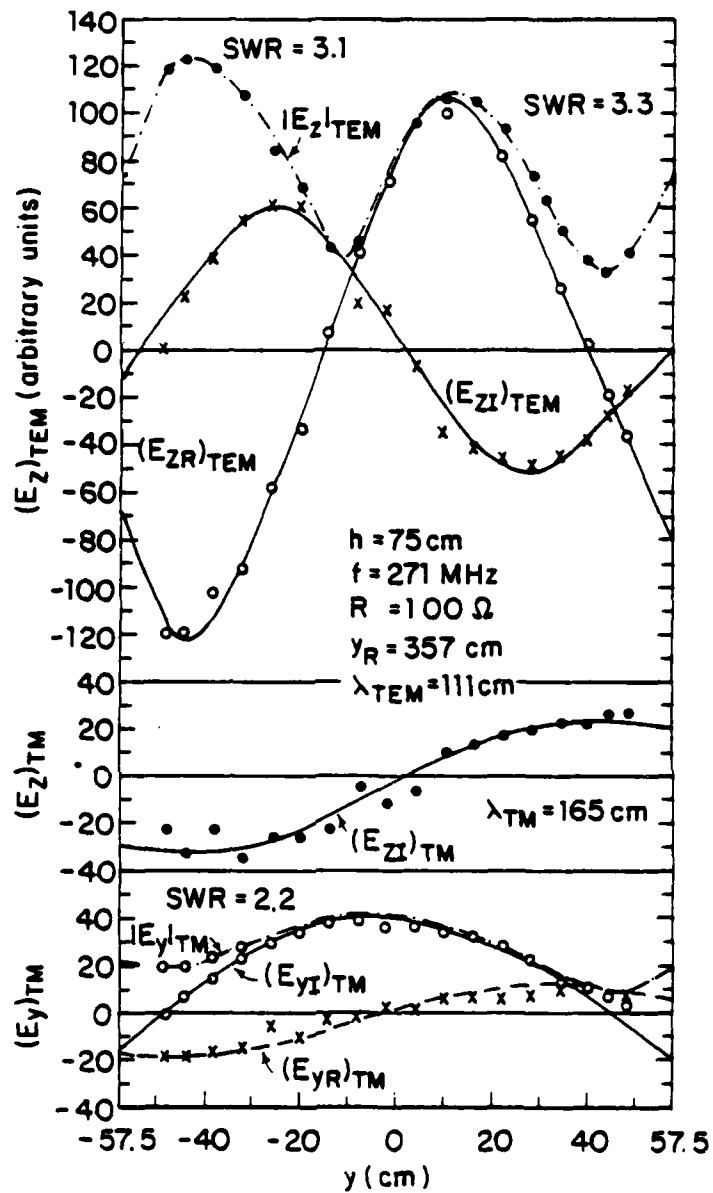


Figure 9. TEM and TM components of the electric field in the parallel-plate region.  $(E_z)_{\text{TEM}} = E_z(z/h = 0.5)$ ;  $(E_z)_{\text{TM}} = E_z(z/h = 0) - E_z(z/h = 0.5)$ ;  $E_z = |E_z| \exp(i\theta_z) = E_{zR} + i E_{zI}$ ;  $\theta_z = 0$  at  $x = y = z = 0$ .

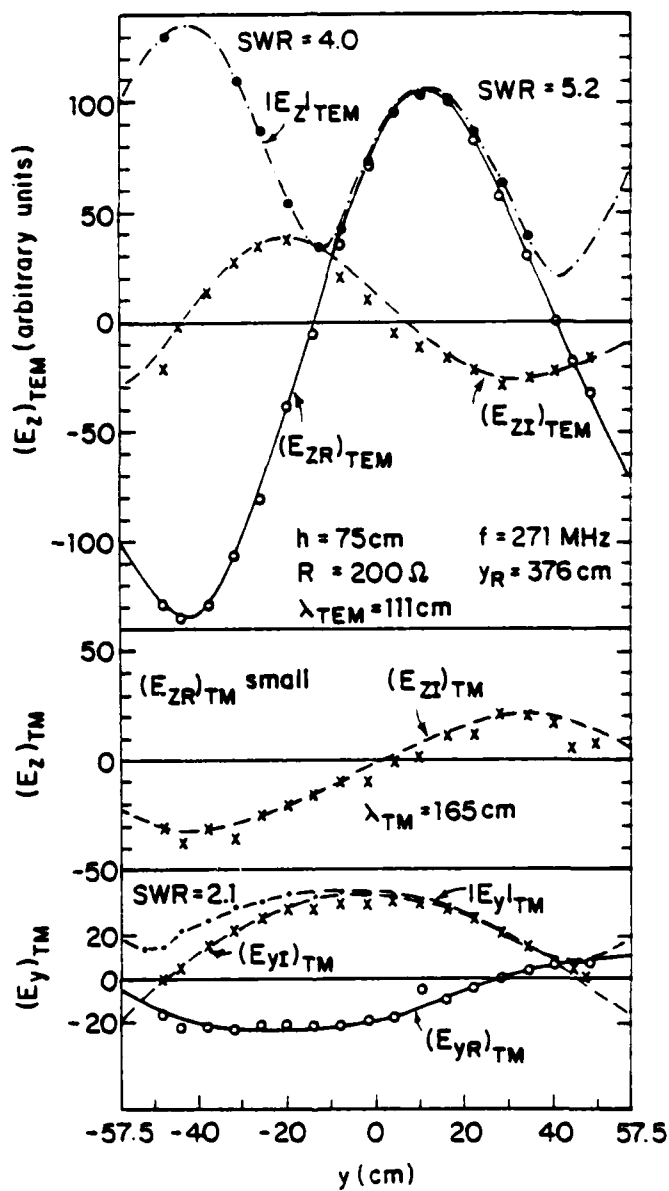


Figure 10. TEM and TM components of the electric field in the parallel-plate region.  $(E_z)_{\text{TEM}} = E_z(z/h=0.5)$ ;  $(E_z)_{\text{TM}} = E_z(z/h=0) - E_z(z/h=0.5)$ ;  $E_z = |E_z| \exp(i\theta_z) = E_{zR} + iE_{zI}$ ;  $\theta_z = 0$  at  $x = z = 0$ ,  $y = 2$  cm.

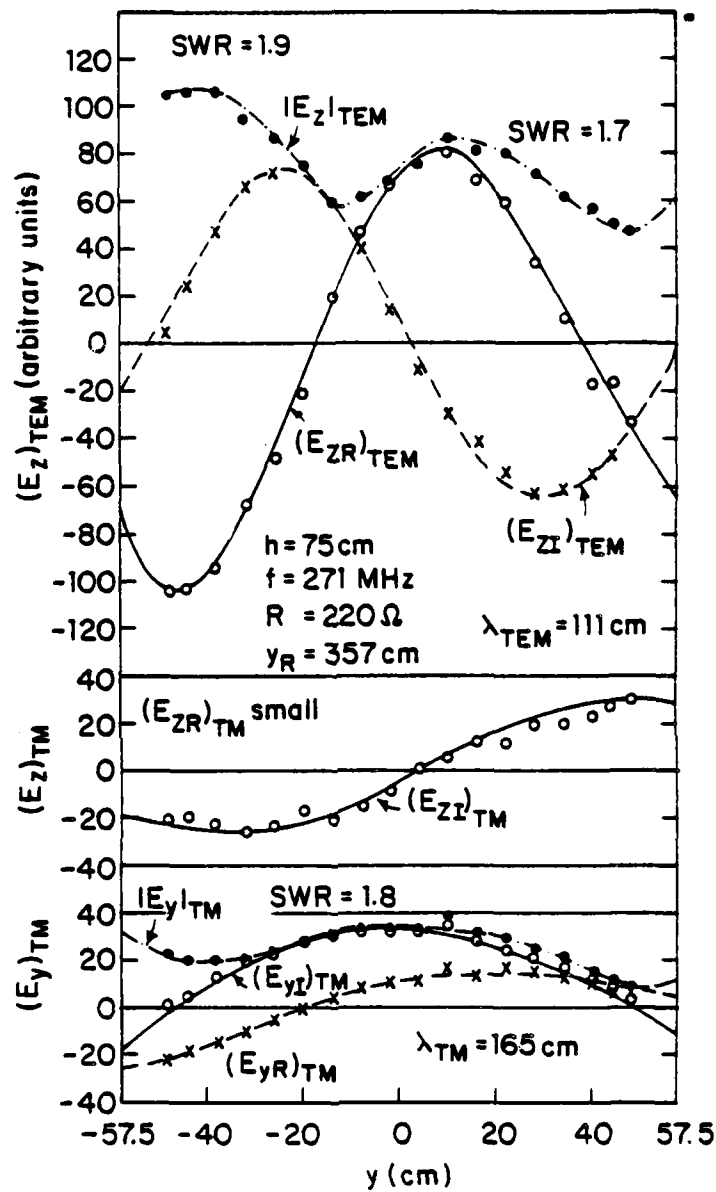


Figure 11. TEM and TM components of the electric field in the parallel-plate region.  $(E_z)_{\text{TEM}} = E_z(z/h=0.5)$ ;  $(E_z)_{\text{TM}} = E_z(z/h=0) - E_z(z/h=0.5)$ ,  $E_z = |E_z| \exp(i\theta_z) = E_{zR} + iE_{zI}$ ;  $\theta_z = 0$  at  $x = z = 0$ ,  $y = 1$  cm.

reaches the resistive termination; most is reflected and radiated at and beyond the end of the parallel-plate region. It is for this reason that the standing-wave ratios with  $R \sim R_c \sim 100 \Omega$  in Figure 8 are virtually the same as those in Figure 10 with  $R \sim 2R_c \sim 200 \Omega$ . It is seen in Figures 9 and 11 that the SWR of the TEM mode alone is reduced substantially below that in Figures 8 and 10 when  $y_R$  is changed from 376 to 357 cm. With  $R \sim 200 \Omega$ , it is reduced from 5.2 to 1.7. The shift from  $y_R = 376$  cm to 357 cm also involves a lengthening of the termination and with it an increase in its inductive reactance. The larger resulting reflection from the termination evidently combines with the reflection at the edge of the parallel-plate region in a phase relation that reduces the SWR. [Similar results have been reported for the full-sized ALECS facility (ref. 3).] The amount of the reduction in the SWR depends on the location  $y_R$  and magnitude of the load resistance  $R$  and the inductance reactance  $L$ . The possible establishment of criteria to determine the optimum values of  $y_R$ ,  $R$  and  $L$  at each frequency requires extensive and systematic series of measurements that are beyond the scope of the present investigation. [The conclusion with regard to the ALECS facility (ref. 3, p. 38) is that the inductance of the terminator should be minimized.]

Also shown in the center in Figures 8 through 11 is the imaginary part of  $(E_z)_{TM}$ . The real part of  $(E_z)_{TM}$  is very small compared with the real parts of  $E_z$  and  $(E_z)_{TEM}$  and, as a small difference between two large quantities, it is difficult to determine accurately; it has been omitted. Of great interest is the imaginary part of  $(E_z)_{TM}$ . Although substantially smaller than the imaginary part of  $(E_z)_{TEM}$ , it can be so located in the standing-wave pattern as to be almost equal and opposite to the imaginary part of  $(E_z)_{TEM}$  precisely where the real part of  $(E_z)_{TEM}$  is zero. When this occurs, a very deep minimum in the total field  $|E_z|$  is produced at this location. Such a cancellation can occur only at widely separated points since the wavelengths of the TEM and TM modes differ significantly. They are 111 cm and 165 cm, respectively.

3. Giri, D. V., Baum, C. E., Wiggins, C. M., Collier, W. O., and Hutchins, R. L., "An Experimental Evaluation and Improvement of the ALECS Terminator," ALECS Memo 8, Air Force Weapons Laboratory, Kirland AFB, NM, 1977.

The component  $(E_y)_{TM}$  in its real and imaginary parts is shown at the bottom in Figures 8 through 11. The larger imaginary part has its maximum at the center. The SWR of the TM mode alone is of the order of 2.

The following conclusions can be drawn from Figures 4 through 11 which apply specifically to  $f = 271$  MHz at which  $h/\lambda = 0.7$ :

(1) The principal contributor to the SWR in the parallel-plate region is the TEM mode. With the simulator matched at low frequencies with  $R \sim R_c \sim 100 \Omega$ , the SWR of the TEM mode is about 5.

(2) A very deep minimum at one location along the ground plane,  $z = 0$ , with a related very high SWR for the total field (up to 27) is due to an almost complete cancellation of the imaginary part of the standing TEM wave by the imaginary part of the standing TM wave precisely where the large real part of the TEM wave goes through zero. This delicate balance can occur only at widely separated points over a limited range of frequencies. The critical conditions which produce the cancellation and the localized deep minimum are readily altered by changes in the position and magnitude of the termination (as from the conditions of Figures 4 and 8 to the conditions of Figures 7 and 11, which reduce the SWR in the total field from 20 to 6.9 with respect to the deep minimum and from 5.6 to 2.5 with respect to the adjacent minimum). Such changes probably merely shift the critical relations to other positions (outside the parallel-plate region) and to other frequencies. They are in any case inadequate in general since they involve a significant change in the terminating resistance and, hence, an undesirable deterioration in the very-low-frequency behavior. However, they do show the possibility of selectively modifying the TM and TEM modes to reduce the SWR of the TEM mode and to eliminate the conditions that create the deep minimum in the total field. It is evidently necessary to devise means to accomplish this at high frequencies without affecting the low-frequency adjustments.

### III. SELECTIVE REFLECTION AND ABSORPTION OF THE TM MODE

A possible method for eliminating the localized very deep minimum and the associated very high SWR is to shift the relative locations of the TEM and TM waves in the standing-wave pattern. This can be accomplished by means of a metal plate that is located halfway between the ground plane and the sloping top plate beginning at the load end of the parallel-plate region. The plate used was 175 cm in the transverse direction and 32 cm in the longitudinal direction. It was inclined to remain halfway between the plates. Since it is located perpendicular to the electric field of the TEM mode, it has no effect on it. For the TM mode, on the other hand, it effectively bifurcates the waveguide and makes each half beyond cut-off. Thus, the plate should strongly reflect the incident TM wave, but let the TEM wave pass without effect.

In Figures 12 and 13 are the measured fields and their separation into TEM and TM modes for precisely the same conditions as those in Figures 4 and 8, except for the addition of the bifurcating plate at the load end of the parallel-plate region that extends into the tapered end section a distance of 32 cm. A comparison of Figures 4 and 12 for the total field shows that the very deep minimum has been eliminated and the SWR of 20.0 in Figure 4 has been reduced to 6.5 in Figure 12; the other minimum has not been affected and the associated SWR is essentially unchanged. It is seen from Figure 13 that the TEM mode is virtually the same as in Figure 8; the bifurcating plate has a minimal effect. On the other hand, the amplitude and location of the imaginary part of the TM wave have been changed. The TM wave is smaller and its maximum is far from the zero of the real part of the TEM wave. As a consequence, the TM mode is largely negligible compared to the TEM mode. The graphs in Figures 12 and 13 when compared with those in Figures 4 and 8 clearly show that the localized deep minimum with an associated very high SWR can be eliminated by suitably reflecting the TM mode while the TEM mode is undisturbed.

It is possible to replace the bifurcating metal sheet by a similarly bifurcating sheet of resistive material in order not merely to reflect the TM mode but to partially absorb it. A detailed analysis of the bifurcating resistive sheet has shown that with a proper choice of surface resistance



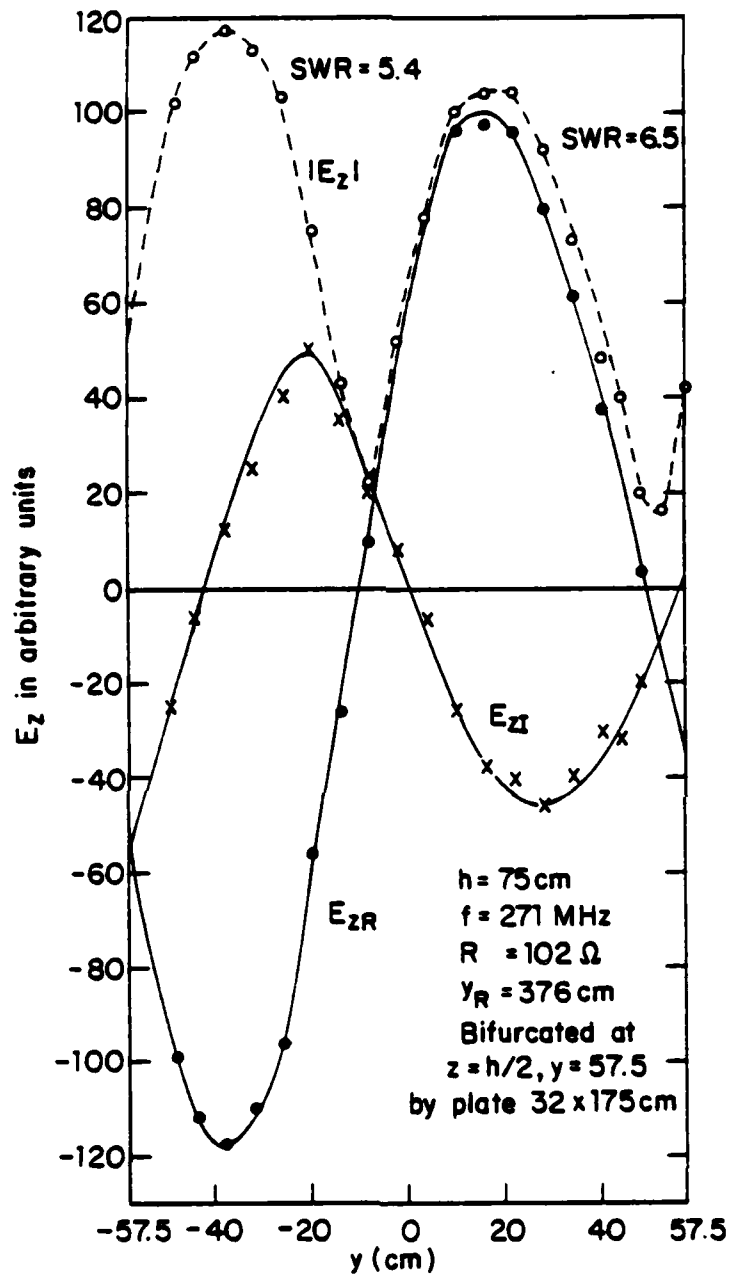


Figure 12. Measured electric field  $E_z = |E_z| \exp(i\theta_z) = E_{zR} + iE_{zI}$ .  
 $\theta_z = 0$  at  $x = z = 0$ ,  $y = 1 \text{ cm}$  on the ground plane.  
 Bifurcating metal plate extending from  $y = 57.5$  to  $y = 89.5 \text{ cm}$ ,  $175 \text{ cm}$  wide.

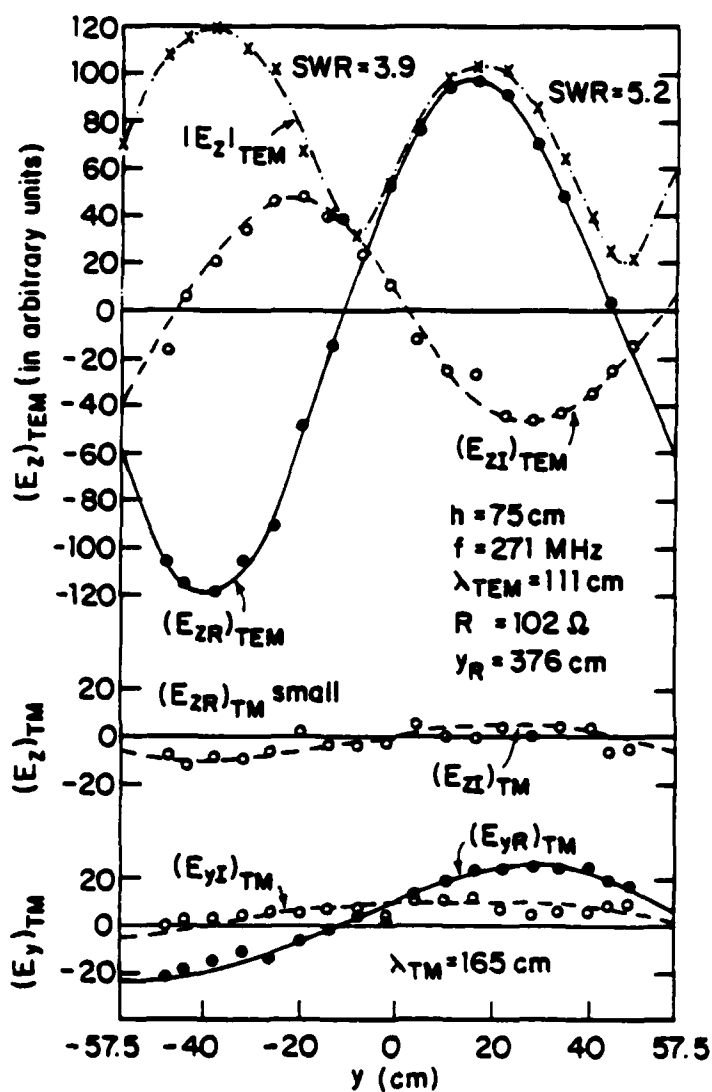


Figure 13. TEM and TM components of the electric field in the parallel-plate region.  $(E_z)_{\text{TEM}} = E_z(z/h = 0.5)$ ;  $(E_z)_{\text{TM}} = E_z(z/h = 0) - E_z(z/h = 0.5)$ ;  $E_z = |E_z| \exp(i\theta_z) = E_{zR} + iE_{zI}$ ;  $\theta_z = 0$  at  $x = z = 0$ ,  $y = 1 \text{ cm}$ . Bifurcated at  $z = h/2$ ,  $y = 57.5 \text{ cm}$  by metal plate ( $32 \text{ cm} \times 175 \text{ cm}$ ).

and length of plate the reflection coefficient for the TM wave can be made very small (ref. 4). However, the reduction in amplitude is frequency-dependent since it involves the electrical length of the sheet.

A modification of the bifurcating resistive sheet consists of layers of resistive sheets arranged throughout the tapered region along surfaces normal to the direction of the electric field due to the TEM mode. Alternatively, strings of suitably spaced resistors can be arranged in place of the resistive sheets in a so-called spatial modal filter (ref. 5) designed specifically to attenuate the TM mode with a minimal effect on the TEM mode. A modal filter of this type was constructed according to the design of Giri and Baum (ref. 6) scaled for the Harvard model simulator. It consisted of 31 generally longitudinal strings of 1/2 Watt resistors with each string composed of 16 resistors in series spaced 7 cm apart. The strings were supported on a styrofoam stand that provided the required semi-ellipsoidal surface characteristic of the equipotentials of the TEM mode. Thus,  $E_{\text{TEM}}$  was everywhere perpendicular to the strings of resistors, while  $E_{\text{TM}}$  was predominantly parallel to them. Measurements made with two different resistances for the elements in the strings, viz., 33  $\Omega$  and 75  $\Omega$ , showed an insignificant reduction in the SWR and, in particular, in the large value due to the "notch." Since it is known that the imaginary part of the TM mode contributes significantly to the formation of the deep minimum or "notch," it appears that the spatial modal filter as constructed is ineffective. Considerably more effective was a single bifurcating sheet, either metallic or resistive.

As shown in Figure 14, the bifurcating metal or resistive sheet is effective in preventing the formation of the deep minimum ("notch") by

4. Shen, H. M., "The Resistive Bifurcated Parallel-Plate Waveguide," IEEE Trans. Microwave Theory & Techniques, MTT-28, pp. 1192-1198, 1980.
5. Giri, D. V., Baum, C. E., and Schilling, H., "Electromagnetic Considerations of a Spatial Modal Filter for Suppression of Non-TEM Modes in the Transmission-Line Type of EMP Simulator," Sensor and Simulation Note 247, Air Force Weapons Laboratory, Kirtland AFB, NM, 1978.
6. Giri, D. V., and Baum, C. E., "Design and Suggested Methods of Evaluating a Spatial Modal Filter," ALECS Memo 11, Air Force Weapons Laboratory, Kirtland AFB, NM, 1979.

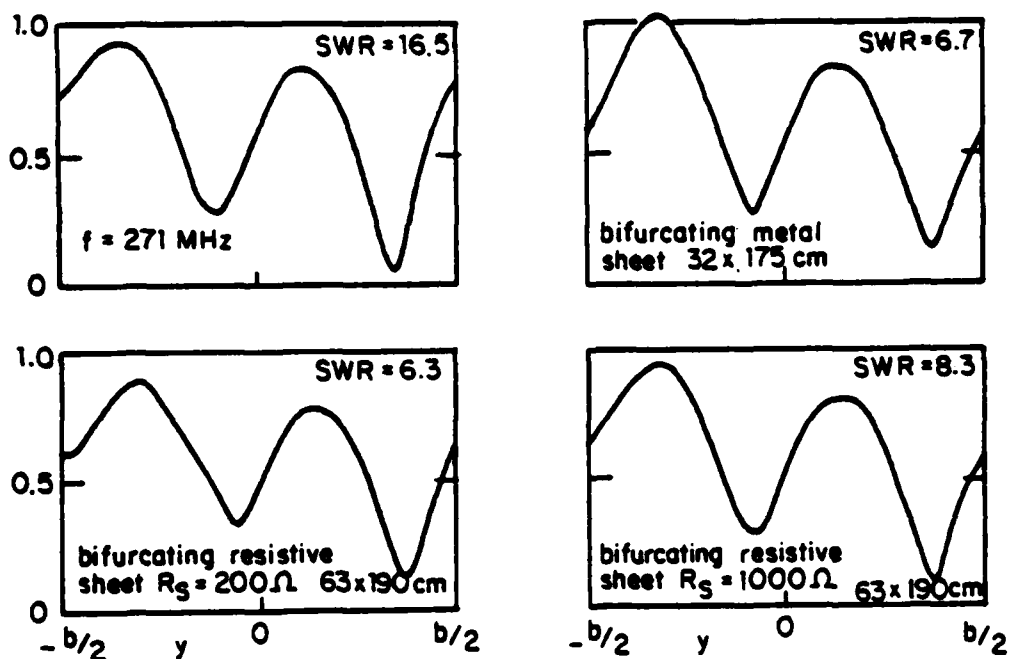


Figure 14. Measured magnitude  $|E_z(0,y,0)|$  of the electric field in the parallel-plate region;  $f = 271$  MHz,  $b = 114.8$  cm,  $h = 75$  cm,  $R = 86 \Omega$ ,  $y_R = 376$  cm.

suitably shifting the TM standing wave relative to that of the TEM mode so that their imaginary parts do not become equal and opposite at any point in the parallel-plate region of the simulator. However, even the complete elimination of the TM mode cannot reduce the large SWR characteristic of the TEM mode in the intermediate range of frequencies.

#### IV. REDUCTION OF THE SWR OF THE TEM MODE

In order to approximate a traveling wave in free space, a simulator must provide an electromagnetic field in its working volume that has a low SWR in the entire frequency band involved in an electromagnetic pulse. Since a properly terminated structure is effective at low frequencies ( $kh \ll 1$ ) and radiation provides a low SWR at high frequencies ( $kh > 2\pi$ ), it remains to reduce the high SWR in the intermediate range ( $kh \sim 2\pi$ ). It has been shown that the deep minimum ("notch") - which provides a locally very high SWR of the order of 20 to 30 - can be eliminated by a suitable shift in the standing-wave pattern of the single TM mode that can propagate at intermediate frequencies. While this is a significant step forward, it leaves unaffected the rather high SWR - of the order of 5 or 6 - of the TEM wave alone. It has been shown that in the central half of the parallel-plate region this can be reduced to 2 by increasing the terminating resistance to two or more times the characteristic resistance and suitably locating it. However, such a change destroys the condition of match at the very important low frequencies. What is required is a device that affects only the intermediate range of frequencies with no effect on the low-frequency properties of the simulator. Such a device can be constructed in the form of a sleeve or apron attached to the tapered section between the parallel plates and the load resistance.

In order to understand the new device, it is well to recall that the standing wave in the electromagnetic field between the two conductors of a transmission line is generated by similar standing waves in the current and charge per unit length in the conductors. Unless these primary currents and charges are closely coupled to the secondary currents and charges in structures (such as spatial modal filters) located between the conductors, such structures necessarily have little effect on the SWR of the primary currents and charges and on the field generated by them. This was shown to be the case for a spatial modal filter constructed of lumped resistors along conductors arranged parallel to a component of the electric field of the TM mode. The new device does not attempt to provide attenuating paths for induced secondary currents on structures located between the conductors of the simulator, but seeks to modify the primary currents directly. This

could be done by cutting the sloping tapered plate leading to the terminating load at some convenient cross section and inserting suitable series impedances to modify the total current - consisting of surface currents on both the inside and outside surfaces of the triangular plate. An experimentally and practically more convenient and probably only slightly less effective method is by means of the equivalent of a fold in the plate itself, as shown in cross section in Figure 15. The structure consists of a trapezoidal plate located parallel to and 5 cm below the triangular plate to form a sleeve or apron with an open end toward the parallel-plate region and a closed end toward the load. The length of the plate between its open and closed ends was varied over a wide range and a length of  $\lambda_{\text{TEM}}/4 = 27.5$  cm was found most effective. The location of the plate (as measured by the distance between its open end and the junction of the triangular-plate and parallel-plate regions) was also varied and a location with  $s = 5$  cm was found effective. Strictly, a similar folded section should be located on the outer as well as on the inner surface of the triangular plate, as suggested by the broken line in Figure 15, since a significant fraction of the total surface current on the triangular plate is on its outer surface. Measurements have shown that the simpler structure consisting of a folded section located only on the inner surface is highly effective, as shown in Figure 16. Attempts to resistively load the apron by means of (1) a parallel bank of relatively low series resistors in place of the short-circuiting end, and (2) a parallel bank of high shunt resistors across the open end did not improve the results. It is to be anticipated that a plate with the length  $\lambda_{\text{TEM}}/2$  with both ends open should have electrical properties similar to those of the apron with the length  $\lambda_{\text{TEM}}/4$  with one end open and the other end closed conductively. Such a change might have structural advantages.

The standing wave in the diagram at the upper left in Figure 16 was measured at the "notch" frequency of 271 MHz before the folded section was attached. The typical deep minimum occurs with an associated SWR of 24. With the folded section inserted with its open end at the junction of the parallel-plate region and the triangular plate ( $s = 0$ ) and its closed end at a distance  $s = 35$  cm from this junction, the standing-wave pattern shown in the middle figure at the top was obtained. Evidently, the "notch" has

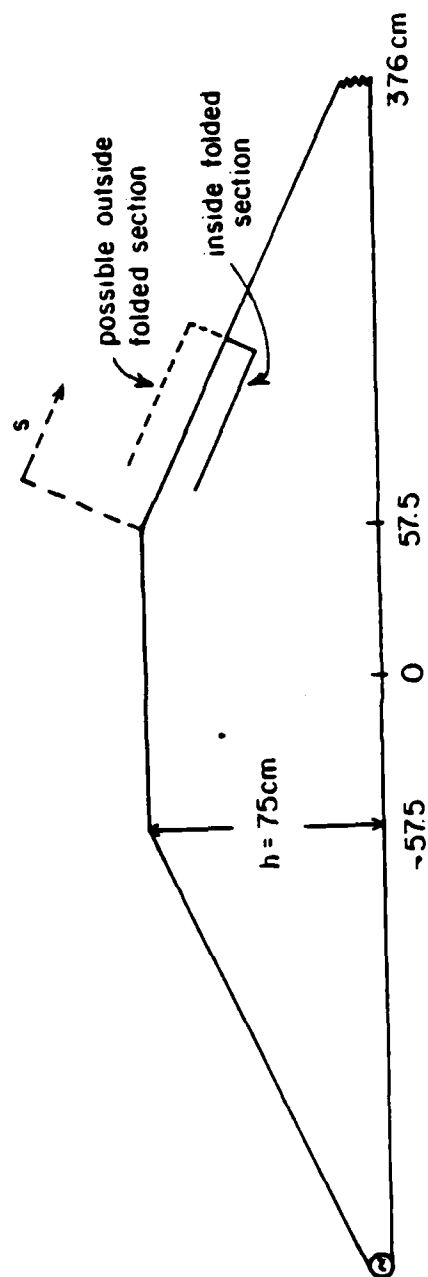


Figure 15. Cross section of Harvard simulator with sleeve or apron sections.



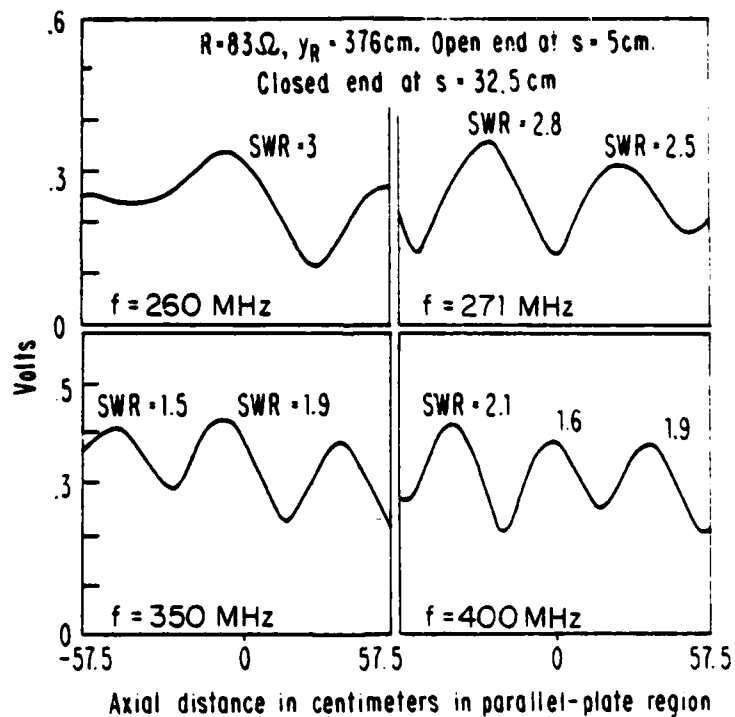
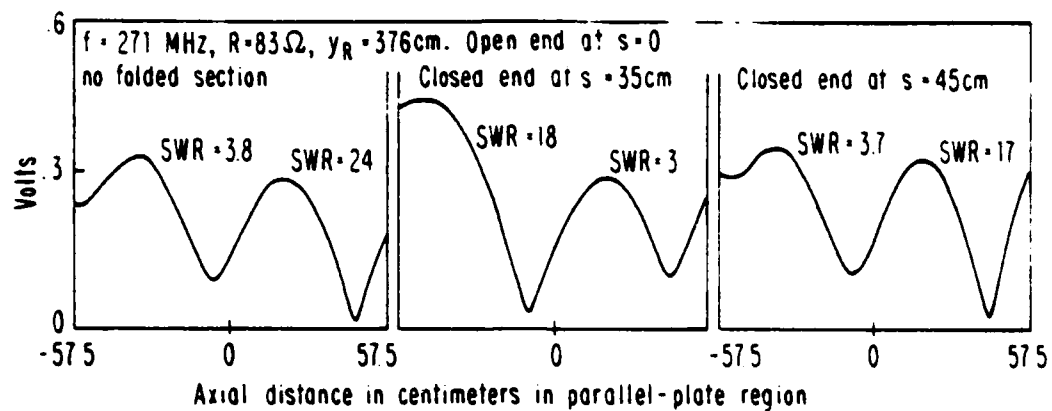


Figure 16. Measured field in parallel-plate region with and without folded section.

been shifted from the second to the first minimum. By lengthening the folded section so that, with its open end at  $s = 0$ , the closed end is at  $s = 45$  cm, the "notch" is shifted back to the second minimum.

The four diagrams in the lower half of Figure 16 were all measured with the folded section located with its open end at  $s = 5$  cm from the parallel-plate and triangular-plate junction at  $s = 0$  and its closed end at  $s = 32.5$  cm so its interior length is  $27.5$  cm  $= \lambda_{\text{TEM}}/4$ . The four graphs are for the frequencies  $f = 260, 271, 350$  and  $400$  MHz. It is seen that no deep minima occur and the SWR is quite low throughout. The SWR at  $f = 200$  MHz was 1.7; at  $f = 450$  MHz it was 2.6.

It may be concluded from these measurements that a folded section or apron of proper length and location can greatly decrease the SWR of the TEM mode over a wide range of frequencies about the "notch" frequency, as well as completely eliminate the notch. Since the apron is most effective when its length from the open end to the short-circuited end is  $\lambda_{\text{TEM}}/4$ , it can be adjusted for maximum effect at the "notch" frequency. As the frequency is decreased, the electrical length and the effectiveness of the apron also decreases. At low frequencies its effect is minimal - the very weak reflection from a small lump of metal. At high frequencies the most important radiation from the structure occurs at the end of the parallel-plate region and this is largely unaffected by anything in the tapered section. Thus, the series apron is effective primarily in a range of frequencies centered about the frequency for which the length of the apron is  $\lambda_{\text{TEM}}/4$ . The conditions leading to an optimum design require more extensive systematic measurements for each simulator.

## V. CONCLUSION

The standing waves generated in the Harvard model simulator have been studied over a wide range of frequencies. It has been verified that in the intermediate frequency range where they are largest, they are due primarily to the TEM mode which experiences reflections before it reaches the termination. This is in contradiction to the assumption in reference 5 (p. 13) that "the dominant TEM mode is a traveling wave because of the matched load at the end whereas the TE and TM modes are standing waves owing to reflections." The deep minimum or "notch" in the electric field has been shown to be due to the almost complete cancellation of the imaginary part of the standing TEM wave by the imaginary part of the standing TM wave near the zero of the real part of the standing TEM wave. The parallel explanation of the deep minimum in the magnetic field given in reference 5 (p. 13) states that "the magnetic field ( $H_x$  component) in the TM modes propagating in the positive and negative  $z$  [our  $y$ ] directions add and their sum [a standing wave] cancels the  $H_x$  component of the principal TEM mode [assumed to be a traveling wave] resulting in the notch behavior." Since a standing TM wave cannot possibly combine with a traveling TEM wave to produce a stationary deep minimum ("notch"), this explanation is meaningful only if the TEM mode that is cancelled consists of a standing wave - which is consistent with experimental observation.

Since the principal contribution to the relatively high SWR in the intermediate frequency range is due to standing TEM waves, even the complete elimination of the TM mode can do no more than remove the "notch" with a negligible effect on the residual, quite large TEM standing wave. Accordingly, a series connected apron has been devised and tested which provides a reflected TEM wave from the tapered region that effectively cancels much of the otherwise reflected TEM wave to leave a greatly reduced SWR in the parallel-plate region. The "notch" is simultaneously eliminated.

The purpose of the experimental studies reported here and in reference 2 has been to obtain a physical understanding of some of the complicated phenomena which occur in EMP simulators. The Harvard model simulator differs from full-sized simulators not only in size but in being constructed of metal plates instead of wire mesh. The same is true of the apron intro-

duced to reduce the SWR. In the full-sized simulator, the apron would presumably also be constructed of wire mesh and in this form should be quite practical. At frequencies for which the mesh size is sufficiently small compared with the wavelength, the differences between the plates and the mesh should not be great.

## LIST OF PUBLICATIONS

### Paper to be Published:

"Standing Waves and Notches in an EMP Simulator and Their Reduction,"  
by R. W. P. King, D. J. Blejer, and T. T. Wu, IEEE Transactions on  
Electromagnetic Compatibility, accepted for publication.

### Talk Presented:

"Analyses of Standing Wave Minima in a Model Simulator,"  
by D. J. Blejer, R. W. P. King, and T. T. Wu, presented at the  
NEM 1980 Conference held in Anaheim, CA, on August 5-7, 1980.

